Purification Mechanism Of HCN By Electrochemically Coupled Copper-Loaded Magnetic Nanoparticles In Liquid Phase Pseudo-Homogeneous System

Guangfei Qu
Kunming University of Science and Technology Faculty of Environmental Science and Engineering
Wei Ji
Kunming University of Science and Technology Faculty of Environmental Science and Engineering
Junyan Li (ljy_2012016@126.com)
Kunming University of Science and Technology https://orcid.org/0000-0002-2553-1620
Shuaiyu Liang
Kunming University of Science and Technology Faculty of Environmental Science and Engineering
Zhishuncheng Li
Kunming University of Science and Technology Faculty of Environmental Science and Engineering
Huimin Tang
Kunming University of Science and Technology Faculty of Environmental Science and Engineering
Junhong Zhou
Kunming University of Science and Technology Faculty of Environmental Science and Engineering
Ping Ning
Kunming University of Science and Technology Faculty of Environmental Science and Engineering

Research Article

Keywords: Electrochemical purification, Magnetic nanoparticles, Transitional-metal, Fenton-like reaction, Purification mechanism

Posted Date: February 22nd, 2022

DOI: https://doi.org/10.21203/rs.3.rs-1233798/v1

Abstract

HCN comes from a wide range of sources, but it is highly toxic and corrosive, harming the environment and human health. This experiment used magnetic nano-Fe_3O_4 particles loaded with Cu were for electrochemical catalytic purification of HCN in a liquid phase pseudo-homogeneous system. The results show that: The purification efficiency of Cu-Fe_3O4 magnetic nanoparticles on HCN is 60% without electricity. After a certain voltage is applied, the purification efficiency of 2h with iron-carbon particles is significantly improved, and the purification efficiency can reach about 95%. And the purification efficiency increases with the increase of voltage. The electrochemical synergistic degradation mechanism of Cu-Fe_3O_4 magnetic nanoparticles is complex, which can directly catalyze the degradation of HCN or form CNO^- intermediates to further degrade into CO_2, H_2O, NH_3, Meanwhile, Fe^{2+}, Cu^+, and other transition metal ions in the liquid phase participate in Fenton-like reaction to further degrade HCN. The results show that the synergistic electrochemical degradation of HCN by Cu-Fe_3O_4 magnetic nanoparticles has excellent potential to purify highly toxic gases.

1. Introduction

HCN is mainly produced in typical industrial waste gas such as coke oven gas, yellow phosphorus tail gas, closed calcium carbide furnace tail gas, and polyacrylonitrile-based carbon fiber (PANCF)(Li et al. 2021a, Wang et al. 2016a). It also comes from electroplating (copper, gold, silver), mining (extraction) Gold, silver), cabin smoking and rodent control industries, or produced as an intermediate product(Brüger et al. 2020, Tan et al. 2009). The existence of HCN hinders the purification and resource utilization of typical industrial waste gas and seriously affects the surrounding environment and human health. After HCN enters the human body through the skin, respiratory tract or digestive tract, it can quickly decompose free cyanide and combine with iron, copper and aluminum in various cellular respiratory enzymes in the human body(Zhang et al. 2021), resulting in metal ions being unable to reduce, thus inactivating the enzyme.

The methods to remove HCN in the gas phase mainly include adsorption, absorption, catalytic oxidation, electrolytic oxidation, etc(Zhou et al. 2019). The absorption method is one of the most widely used and mature methods in the industry. In this method, the waste gas containing HCN is first absorbed through lye to generate CN^-, and then the CN^- is treated and converted into non-toxic and harmless substances, and then discharged(Shi et al. 2015). The electrolytic oxidation method takes graphite as anode and iron plate as the cathode. The waste liquid containing cyanide ions is added into the electrolytic cell, and the simple cyanide and complex in the wastewater are oxidized into cyanate, N_2 and CO_2 by direct current(Xie et al. 2018). When the cyanide content is low ([CN^-]<500mg/L), salt can be added to increase the electrolyte concentration. When [CN^-] >500mg/L, electrolysis can be carried out directly, but the discharge standard cannot be reached after one treatment, and further treatment is required. The problem of the electrolytic oxidation method is that the electrolytic efficiency is not stable, easy to produce harmful gas, high treatment cost.

Microelectrolysis is also called iron-carbon internal electrolysis technology. By adding an appropriate proportion of iron particles and carbon particles to sewage, a tiny galvanic cell is formed between iron particles and carbon particles under the action of the electric field, with iron particles as the anode and carbon particles as the cathode(Li et al. 2021b, Wang et al. 2016b). In addition, Fe^{2+}, Fe^{3+} and OH^- in the solution can generate $Fe(OH)_3$, $Fe_3[Fe(CN)_6]_2$, $Fe_4[Fe(CN)_6]_3$ and other flocculants, which can further remove pollutants through adsorption, flocculation and sedimentation, and also have decolorization function(Huong et al. 2021, Xiao et al. 2021). However, microelectrolysis technology is mainly used in the purification of organic wastewater, and there are few studies on the degradation of inorganic gaseous pollutants such as HCN.

In recent years, many researchers, especially those in the field of organic synthesis, have devoted themselves to loading homogeneous catalytic active components such as platinum, palladium, copper, etc. on the surface of magnetic nano-Fe_3O_4 to prepare stable and recyclable heterogeneous catalysts(Gawande et al. 2013), this type of catalyst is widely used in green chemistry and environmentally friendly catalysis(Aliaga et al. 2010). However, there is no report on the use of magnetic nanocatalysts loaded with single metal or bimetal to purify HCN in a pseudo-homogeneous system.

In this study, magnetic nano-Fe_3O_4 particles were prepared and the active component Cu was loaded on them. Under the action of the electric field, it was combined with micro-electrolysis technology for the purification of HCN. According to the gas purification situation of supported magnetic nano-catalyst, a catalyst with purification potential could be invented.

2. Materials And Methods

2.1 Materials

The main reagents used in the experiment are analytical reagents, and the experimental water is all prepared with deionized water. Use gas flow meters to measure and control the usage of gas (HCN), oxygen (O_2) and carrier gas (N_2). Nitrogen and oxygen are high purity gases, with a content of 99.999%. The concentration of HCN gas is 500ppm, and the remaining gas is nitrogen. The iron-carbon particles were purchased from Shandong Yingkelinchuan Environmental Protection Technology Co., LTD. The proportion is 1.1t/m^3, the specific surface area is 1.2m^2/g, and the porosity is 65%. Its chemical composition is Fe80% and C20%, and it is repeatedly washed with deionized water before use.

2.2 Experiment device

Experimental equipment and process are shown in Fig. 1. The main reaction device is a bubble reactor, the reaction medium is deionized water, 316L stainless steel as anode and carbon rod as the cathode. Iron-carbon particles and self-made magnetic Fe_3O_4 nanoparticles loaded with copper are mixed in a certain proportion, and then added into the reactor for electrochemical reaction under different voltages. The gas used in the experiment is cylinder gas, and dynamic simulation gas distribution is adopted. The

gas components HCN, O_2 and N_2 to be treated are mixed into the gas mixing tank according to a certain metering ratio, and then into the reactor for reaction. The tail gas from the reactor is treated by the tail gas absorption device and discharged. Gas sampling points are set at the inlet and outlet of the reactor respectively, and sampling and analysis are performed at a certain interval. At the end of the reaction, magnetic solid-liquid separation and characterization.

2.3 Preparation of magnetic Cu-Fe_3O_4 nanoparticles

2.3.1 Preparation of nano-magnetic Fe_3O_4 particles

Nano-magnetic Fe_3O_4 particles are prepared by the reverse co-precipitation method(Aono et al. 2005). Weigh an appropriate amount of $FeCl_2 \cdot 4H_2O$ and $FeCl_3 \cdot 6H_2O$ (wherein, the molar ratio of ferrous salt to iron salt is 1:2, and the actual amount of ferrous salt may be slightly excessive when weighing), and an appropriate amount of citric acid, 0.85 mL of concentrated hydrochloric acid was added to 25 mL of deionized water after deoxygenation treatment, and then 5.2 g of $FeCl_3$ and an appropriate amount of $FeCl_2$ were added in sequence to fully dissolve to obtain a mixed solution. Then, under vigorous stirring, the resulting solution was added dropwise to 250 mL 1.5mol/L NaOH solution. During this period, a large amount of black sol can be observed to form rapidly. The mixed system was crystallized at room temperature for 30 minutes, the magnet was separated, washed with deoxygenated and deionized water to neutrality, soluble ions were removed, and vacuum dried to obtain ultrafine powdered Fe_3O_4.

2.3.2 Preparation of Cu-Fe_3O_4

Disperse the Fe_3O_4 prepared by the reverse coprecipitation method in the liquid phase(Cano et al. 2012), add a concentration of $CuCl_2$ solution, stir in a constant temperature water bath at 25±1°C for about 10 minutes. To adjust the pH values of the working solution dilute NaOH solution was used. The reaction was carried out under stirring at room temperature for 24 hours. After magnetic separation, washing to neutrality, dried in vacuum at 60° C. To obtain magnetic Fe_3O_4 nanoparticles loaded with copper.

2.4 Calculation of experimental result

The calculation formula of HCN removal rate is shown in (1):

$$\eta = (C_i - C_0)/C_i \quad (1)$$

In formula (1), C_i and C_0 are the content before and after HCN, and the removal amount is mg/m^3.

3. Results And Discussion

3.1 Characterization of magnetic nanoparticles

3.1.1. TEM analysis

Figure 2(a) is the TEM image of Cu-Fe_3O_4 magnetic nanoparticles. It can be seen from the TEM that the grains of Cu-Fe_3O_4 magnetic nanoparticles are mostly spherical or spheric-like, and the grain size is relatively uniform(Meng et al. 2005, Vijayakumar et al. 2000). Spherical or spheric-like nanoparticles have a large specific surface area, which is conducive to improving the surface activity of the Cu-Fe_3O_4 nanocatalyst. It can be seen from the EDS test results: copper was successfully loaded on the magnetic nanoparticles. The loading capacity was slightly higher than the theoretical loading capacity, which may be due to the residual Cu^{2+} ions in the solution on the surface of nanoparticles.

3.1.2 XRD test

To explore the loading components of the loaded nanoparticles, XRD characterization was carried out. According to the XRD peaks of the samples synthesized by the anti-coprecipitate method, as shown in Fig. 2(b), corresponding to PDF card 19-0629, the synthesized samples were confirmed to be magnetic nanoparticles Fe_3O_4. The half-height and width of the strongest peak of the sample were calculated by the Debye-Scherrer formula (1), so the grain size of Fe_3O_4 prepared by the reverse coprecipitation method was 13.5nm.

$D = 0.89\lambda / \beta \cos\theta$ (2)

In formula (2), λ is the X-ray wavelength and D is the grain diameter.

The diffraction peaks of loaded and unloaded nanoparticles at 2θ = 30.1°, 35.5°, 43.1°, 57.0° and 62.7° correspond to planes 220, 311, 222, 422 and 511 of the face-centered cubic structure Fe_3O_4(Nikazar et al. 2014), which are the characteristic peaks of Fe_3O_4. According to the XRD patterns of the loaded components of magnetic Fe_3O_4, the loaded catalysts were not damaged by the loaded transition metal. However, Cu has no obvious corresponding diffraction peak of metal oxide, which indicates that Cu is difficult to be detected in uniform and less dispersed microcrystals.

The intensity of the main diffraction peak of magnetic Fe_3O_4 decreases with the introduction of Cu, which may be because the metal compound has a higher absorption coefficient of X-ray so that the X-ray absorbed by Cu and the intensity of the corresponding main diffraction peak decreases. At the same time, the diffraction peak of magnetic Fe_3O_4 becomes wider after loading copper, indicating that the grain size becomes larger after loading copper, and vice versa. This result can be interpreted that the dispersion of magnetic Fe_3O_4 is improved after loading copper.

3.1.3 BET analysis and potential test

After the composition was determined, the pore size, particle size and potential of Cu-Fe_3O_4 nanoparticles before and after loading were tested. The specific surface area and pore volume of magnetic nanoFe_3O_4 loaded with Cu were tested by BET, and the Zata potential on its surface was measured to analyze the dispersion among nanoparticles. The results are shown in Table 1.

Table 1
Pore size, particle size and zeta of Fe_3O_4 loaded with copper before and after loading

Sample	Pore/nm			Malvern	
	adsorption	desorption	Average pore diameter	Particle/nm	Zeta/mV
Unloaded	1.234	9.732	9.0137	476.2	-11.9
Cu-loaded	0.8235	5.092	7.75042	490.4	-28.0

The results show that the preparation of nanoparticles is negatively charged surface, the surface of the nanoparticles after load average potential absolute value is higher than before the load, and the highest potential absolute value of a load of copper, for 28 mv, the potential absolute value is close to 30 mv, Zeta potential increased to reduce the phenomenon of reunion, increased the system stability, better dispersion(Crundwell 2016), It is consistent with XRD results. However, the Zeta potential of the studied system is also affected by other factors, such as the change of the pH value of the dispersion system, the change of the conductivity of the solution, and the concentration of surfactant, among which the most important factor is the pH value(Hong et al. 2019). In the experimental process, the Zeta potential of the actual reaction system was not involved too much due to the test conditions.

Compared with N_2-BET and particle size analysis, the total pore volume of the magnetic nanoparticles loaded with copper is 0.3165 cc/g, and the surface area is 167.683 m^2/g, indicating that the magnetic nanoparticles loaded with Copper have a larger specific surface area, while the average pore size decreases, which is more favorable for the adsorption reaction of gas on the particle surface.

3.2 Cu-Fe_3O_4 magnetic particles removal of HCN

3.2.1 Cu-Fe_3O_4 catalyzed degradation of HCN in pseudo-homogeneous liquid phase

Cu-Fe_3O_4 liquid phase catalytic degradation of HCN without applying voltage: A certain amount of Cu-Fe_3O_4 magnetic nanoparticles were measured and dispersed in the reactor. HCN gas with a certain O_2 was injected at the bottom of the reactor and the purified gas was discharged from the top of the reactor. The gas products were collected during the reaction. After the reaction, magnetic solid-liquid separation was performed to characterize the gas, liquid and solid samples. Reaction conditions: initial pH 6.00±0.01 and T=25°C, initial concentration of HCN were 200ppm, the gas flow was 300ml/min, a small amount of catalyst Cu-Fe_3O_4.

HCN degradation results are shown in Fig. 3(a). The purification effect of Cu-loaded Fe_3O_4 magnetic nanoparticles is significant. Within 100min, HCN decreases rapidly and then gradually decreases. The purification efficiency is stable above 70%, which is better than that of the control group.

The gas after the reaction was analyzed by gas chromatography for decomposition products, and the results were shown in Fig. 3(b): There is a small spike near the O_2+N_2 peak, which is calibrated as CO_2. Since a mixture of N_2-HCN and a certain concentration of O_2 is passed into the reaction system, the reaction system is closed, there is no source of CO_2, and the only C-containing substance is HCN, so it can be judged that CO_2 is the product of HCN oxidation. The proportion of O_2+N_2 in the mixed gas is very large, and its chromatographic peak and CO_2 peak cross, so the CO_2 quantitative calibration result is too small.

The inlet gases were N_2, HCN and O_2 before the reaction, and there was no source of CO_2 in the inlet. However, more NH_3 and CO_2 were detected in the products after the reaction, and the proportion of N_2 increased. It can be seen that the products of HCN purified by loaded Cu nanoparticles include CO_2, N_2 and NH_3.

The reaction takes place in solution, and part of HCN is directly oxidized to CO_2 and N_2 under the action of Cu-Fe_3O_4 magnetic nanoparticles(Liu et al. 2021, Yin et al. 2021). The reaction formula is as follows:

$$4HCN+5O_2 \rightarrow 4CO_2+2N_2+2H_2O \quad (3)$$

$$3HCN+3O_2 \rightarrow 3CO_2+N_2+NH_3 \quad (4)$$

$$2HCN+2O_2 \rightarrow CO_2+CO+N_2+H_2O \quad (5)$$

The Gibbs free energy of the related reaction equation is calculated, and the order of Gibbs free energy is: (3)>(4)>(5). It can be seen that reaction (3) and (4) are the main reactions and contribute the most to the products, while the contribution of reaction formula (5) is small, so the content of CO in the reaction products is low and cannot be detected.

To further explore the changes of Cu-Fe_3O_4 magnetic nanoparticles during the reaction, the Raman test was carried out on the magnetic nanoparticles after the reaction. According to The Raman test in Fig. 3(c), it can be seen that the characteristic peak value of Fe_3O_4 decreases at 278cm^{-1}, 389cm^{-1} and 680cm^{-1}, which is because the signal of the iron element is relatively reduced after the loading of copper. In the process of static purification of HCN, magnetic nanoparticles dissolve some metal elements into the liquid phase. In the liquid phase dissolved state participate in the reaction, but due to low sensitivity, so not detected. ICP inductively coupled plasma analysis showed that 2.183μg/mL copper and 6.477μg/mL iron were found in the supernatant after the static reaction of Cu-loaded magnetic nanoparticles with HCN. Specific reactions are as follows:

$$HCN(g) \rightarrow HCN(l) \rightarrow CN^- + H^+ \quad (6)$$

$$4CN^- + Cu^+ \rightarrow [Cu(CN)_4]^{3-} \quad (7)$$

$8HCN+Fe_3O_4=Fe(CN)_2+2Fe(CN)_3+4H_2O$ (8)

$3Fe^{2+}+6CN^- \rightarrow Fe_2[Fe(CN)_6]$ (9)

Due to the low content of iron in the solution, $Fe(CN)_2$, $Fe(CN)_3$, $[Cu(CN)_4]^{3-}$ are formed only in the form of macromolecular colloidal particles, which are not easy to flocculate and precipitate.

To explore the changes of elemental groups in the liquid, the magnetic particles before and after loading Cu were used to purify HCN liquid for FT-IR analysis. The FT-IR analysis results are shown in Fig. 3(d). At 2100~2200cm^{-1}, an obvious CN^- absorption peak appears, indicating that part of CN^- appears in the liquid after the reaction of HCN with Cu-loaded magnetic particles. However, due to the low copper content in the solution, The characteristic peak of 918-923 cm^{-1} attributed to Cu^{2+} and the peak of copper oxide were not detected in the infrared spectrum(Siddiqui et al. 2016). The infrared spectrum at 3200-3800cm^{-1} is to characterize the stretching vibration of -OH, and the obvious wide peak at 3452cm^{-1} is mainly due to the vibration of -OH generated by water or hydroxide in the reactant.

3.2.3 Electrochemical catalytic degradation of HCN with Cu-Fe3O4 in pseudo-homogeneous liquid phase

Considering the high toxicity of HCN and to facilitate the detection and analysis of the products, deionized water and a certain amount of Cu-Fe_3O_4 magnetic nanoparticles were added to the reactor as the reaction medium. After victimization, HCN was passed through, and HCN gas was first absorbed in the liquid phase. Then, the influence of voltage and reaction time on the removal effect under different conditions such as electrolysis, electrolysis + aeration, electrolysis + micro-electrolysis, electrolysis + micro-electrolysis + aeration is discussed. The removal rate is converted according to the difference of component concentration before and after the reaction. Under the above reaction conditions, the reaction was conducted for 2h under different voltages (0.8, 1.0, 1.5, 1.9 and 2.5V), respectively. The removal effects of electrolysis, electrolysis + aeration, electrolysis + micro-electrolysis, electrolysis + micro-electrolysis + aeration and other conditions are shown in Fig. 4(a).

It can be seen from Fig. 4(a) that in the same reaction time, the increase of voltage contributes to the degradation of HCN. Under different voltages, the order of purification effect is as follows: electrolysis + micro-electrolysis + aeration > electrolysis + micro-electrolysis > electrolysis + aeration > electrolysis + micro-electrolysis + aeration. The degradation efficiency of HCN in the electrolysis + micro-electrolysis + aeration group is significant, but there is little difference between electrolysis and electrolysis aeration. When the voltage increases from 1.0V to 1.5V, the purification effect of electrolysis + micro-electrolysis increases significantly compared with electrolysis and electrolysis aeration. The removal rate at 1.5V is more than 85%, and the gap between the purification effect of electrolysis + micro-electrolysis + aeration decreases gradually. The purification effect of electrolysis + micro-electrolysis and electrolysis + micro-electrolysis + aeration (especially electrolysis + micro-electrolysis + aeration) increases gradually when the voltage is greater than 1.5V. Thus the addition of iron-carbon particles on the electrochemical

degradation of HCN has an obvious effect, the reason may be that the addition of iron-carbon particles uniform discharge reaction system, forming a micro-electric field in the surface of the iron-carbon particles, each of the iron-carbon particles surfaces micro reaction area, at the same time, iron-carbon particles and Cu-Fe_3O_4 magnetic nanoparticles mixing in the system, contact closely, Reduce the distance between the reacting substances. Then, with the increase of voltage, the system without iron and carbon particles can also form a uniform and stable electric field under the electric field stimulation, which increases the degradation rate of HCN.

Because after the voltage of 1.5 V, the degradation rate was significantly increased in each group, increasing the voltage degradation efficiency after little change, at the same time, from the angle of the combination of reaction conditions, when other things being equal, pure electrolytic purification effect of HCN is limited, if you want to achieve a better removal effect electrolysis voltage may be increased, but this will no doubt increase the power consumption, both purification efficiency and power consumption of two ways, 1.5V was selected for subsequent experiments.

Figure 4(b) shows the removal effect of HCN at 1.5V voltage for different reaction periods. As can be seen from the figure, with the extension of reaction time, the purification effect of A, B, C and D is getting better and better, and the differences among the four gradually narrow. When the reaction time was 5h, the removal rate was more than 95%. When the reaction time is less than 4h, the purification effect decreases in the order of D, C, B and A at the same time. There is little difference between the purification effect of D and C, and the purification effect of B and A, but the effect of the former two is significantly better than the latter two, especially when the reaction 2h, the difference is the largest (C is more than 85%, while B is less than 60%). These results indicate that Cu-Fe_3O_4 magnetic nanoparticles have a significant degradation efficiency of HCN under the synergistic effect of iron and carbon particles micro-electrolysis. When the reaction time increased from 2h to 5h, the purification efficiency of D did not increase significantly. In the same reaction time, the removal effect changes in the order of electrolysis + micro-electrolysis + aeration > electrolysis + micro-electrolysis > electrolysis + aeration > electrolysis. Especially for 1h reaction, the removal rate of HCN by electrolysis + micro-electrolysis + aeration is close to 60%, which is much higher than 12% by pure electrolysis, indicating that certain purification effects can be achieved in a short time under combined conditions. To a certain extent, this indicates that in the actual treatment of HCN gas, due to the continuous flow of gas into the reaction system, a certain removal rate can be achieved under the condition of limited residence time.

The gas products of HCN were degraded by electrolysis + Microelectrolysis + aeration for chromatographic analysis, and the results were shown in Fig. 4(c). The carrier gas used is N_2, and the gas composition mainly consists of H_2, O_2 and a small amount of CO_2. The wide peak corresponding to the retention time of 14.767min is presumed to be a water leak, which has not been calibrated due to limited conditions. During the reaction process, H_2 and O_2 are precipitated in cathodic and anodic electrolysis respectively. The theoretical ratio of H_2 and O_2 is 2:1, but the actual ratio is close to 1, which may be caused by the mixing of O_2 in the mixture entering the system. The reaction system is closed, and there is

no CO_2 in the system. The only source of CO_2 may be generated after the HCN reaction. The reaction takes water as the medium, and the CO_2 produced spills out of the system with airflow. No peaks of other gas components were detected, so it can be inferred that HCN mixture gas is oxidized to CO_2 and N_2 through a series of complex reactions under the joint action of O_2 in the mixed flow and reactive oxygen species generated by electrolysis after entering the liquid phase.

3.3 reaction mechanism

Electrochemistry works with Cu-Fe_3O_4 magnetic nanoparticles to purify HCN gas. Under the catalysis of Cu-Fe_3O_4 magnetic nanoparticles, the addition of electrochemistry greatly reduces the activation energy of the reaction and improves the reaction efficiency. Meanwhile, the addition of iron-carbon microelectrode forms numerous micro-discharge regions, and the electric field distribution in the reactor is more uniform. It can achieve a higher purification effect under smaller voltage and reduce energy consumption. A complete active region was formed between each pair of iron and carbon particles to reduce the reaction distance of HCN and enhance the transfer rate of HCN in the reactor. A single pair of microelectronic fields composed of iron-carbon particles was taken as a unit element to form a complex reaction chain in the whole reaction system. The pseudo-homogeneous reaction mechanism of the electrochemical coordination of Cu-Fe_3O_4 magnetic nanoparticles was analyzed by taking a single unit element of the microelectronic field as an example.

Its reaction mechanism is shown in Fig. 5:

Under the combined action of oxygen and electric field, the HCN degradation reaction is strengthened. In addition to direct oxidation (reaction 3-5), CNO intermediates(Li &Sarathy 2020, Öğütveren et al. 1999) are also generated during the HCN degradation process, which is further oxidized into CO_2, N_2 and H_2O under the action of the catalyst. reactions are as follows:

$2HCN+O_2 \rightarrow 2CONH$ (10)

$2CONH+O_2 \rightarrow CO_2+H_2O+N_2+CO$ (11)

In the anode zone:

$CN^- + 2OH^- - 2e^- \rightarrow CNO^- + H_2O$ (12)

$2CNO^- + 4OH^- - 6e^- \rightarrow 2CO_2 + N_2 + 2H_2O$ (13)

$2CN^- + O_2 \rightarrow 2CNO^-$ (14)

$2CNO^- + O_2 - 2e^- \rightarrow 2CO_2 + N_2$ (15)

In addition, CN^- loses electrons at the anode and is oxidized to acid radical, which is further oxidized to CO_2, H_2O(Abdel-Rahman et al. 2019, Liu et al. 2021, Zhu et al. 2019), etc:

$2CN^{-}-2e^{-}\rightarrow(CN)_2$ (16)

$(CN)_2+4H_2O\rightarrow(COO)_2^{2-}+2NH^{4+}$ (17)

$(COO)_2^{2-}+4NH^{4+}\rightarrow2HCOOH+4NH_3-2e^{-}$ (18)

In the cathode zone, With the participation of oxygen, H_2O_2 will be generated in the cathode region as follows:

$O_2+2H_2O+2e^{-}\rightarrow HO_2^{-}+OH^{-}$ (19)

$HO_2^{-}+H_2O+2e^{-}\rightarrow H_2O_2+OH^{-}$ (20)

H_2O_2 produced in the system can also react with Cu^{+} and Fe^{2+} in the solution (under alkaline conditions) to generate hydroxyl radicals:

$Fe^{2+}+H_2O_2\rightarrow Fe^{3+}+\bullet OH+OH^{-}$ (21)

$2Cu^{+}+H_2O_2\rightarrow 2Cu^{2+}+\bullet OH+OH^{-}$ (22)

Because ·OH and H_2O_2 both have strong oxidation capacity, part of HCN is removed by oxidation reaction under the action of ·OH. At the same time, after oxidation, the obtained Cu^{2+} and Fe^{3+} ions are reduced to Cu^{+} and Fe^{2+} after electron gain at the cathode, which makes the Fenton reaction continue and produce a large amount of ·OH.

In addition, after the reaction, the color of the solution changed from colorless to light brown. After the detection of Fe^{3+}, the potential difference between iron and carbon in the iron-carbon particles formed countless tiny galvanic cells, in which the iron was corroded into divalent iron ions into the solution. The results indicate that the electrode directly and indirectly participates in the reaction under-voltage and micro-electrolysis:

$Fe-2e^{-}\rightarrow Fe^{2+}$ $E(Fe/\ Fe^{2+})=0.44V$ (23)

$Fe^{2+}+O_2+4H^{+}\rightarrow2H_2O+Fe^{3+}$ (24)

$3Fe^{2+}+6CN^{-}\rightarrow Fe_2[Fe(CN)_6]$ (25)

$Fe_2[Fe(CN)_6]+2H_2O_2+4H^{+}\rightarrow Fe_4[Fe(CN)_6]3+2Fe^{2+}+4H_2O$ (26)

$Cu^{+}+4CN^{-}\rightarrow[Cu(CN)_4]^{3-}$ (27)

It has been found that in the presence of copper cyanide complex, H_2O_2 can oxidize Cu^+ in $[Cu(CN)_3]^{2-}$ and $[Cu(CN)_2]^-$ to Cu^{2+} and generate CNO^- at the same time(Nguyen et al. 2013). The reaction process is as follows:

$2[Cu(CN)_3]^{2-}+H_2O_2+3O_2 \rightarrow 2Cu^{2+}+6CNO^-+2OH^-$ (28)

Similarly, the complex formed by Fe^{2+} and CN^- also has a similar reaction:

$2Fe(CN)_2+H_2O_2+2O_2 \rightarrow 2Fe^{3+}+4CNO^-+2OH^-$ (29)

4. Conclusion

In the liquid phase pseudo-homogeneous reaction system, the purification effect of Cu-Fe_3O_4 magnetic nanoparticles was significantly increased under the action of the electric field. With the increase of voltage, the electric field in the reaction chamber without micro-electrolysis was gradually uniform, and the purification effect was greatly improved. The addition of iron and carbon micro-electrolysis is conducive to the uniform distribution of electric field, reducing the reaction path, and more conducive to the degradation of HCN, to achieve efficient degradation of HCN under low voltage.

The degradation mechanism of HCN was further analyzed by using a unit micro-electric field composed of a single pair of iron and carbon Microelectrolysis. The study showed that the degradation reaction of HCN was complex, which could be directly degraded by Cu-Fe_3O_4 magnetic nanoparticles or catalyzed by the formation of intermediate product CNO^-, and further degraded by Fenton reaction to generate highly active hydroxyl radicals and H_2O_2. In the solution, Fe^{2+} and Cu^+ electrons were reduced to their original state at the cathode to participate in the Fenton reaction again, resulting in continuous generation of highly active hydroxyl radicals and further degradation of HCN. The complexes formed by various metal ions and CN^- participate in the reaction under electrolysis, and finally achieve the complete degradation of HCN.

Electrochemical degradation of HCN with Cu-Fe_3O_4 magnetic nanoparticles can effectively degrade HCN in industrial waste gas to a certain extent, but the degradation process is highly dependent on O_2, and the degradation of HCN with low O_2 content or without O_2 needs further study. Due to Cu - Fe_3O_4 nanoparticles having certain magnetic, can further recovery was achieved by an external magnetic field, or by changing the magnetic field direction and size of catalyst in the environment of mobile, through further research on Cu-control of the magnetic Fe_3O_4 nanoparticles and mobility, catalytic control precision, has wide industrial application prospect.

Statements And Declarations

Funding

This work was supported by the National Key Research and Development Program of China. (Grant No.2018YFC1900203)

Competing interests

The authors declared that they have no conflicts of interest to this work.

Authors' contributions

Guangfei Qu: Conceptualization, Methodology, Investigation, Writing - Original Draft; **Wei Ji:** Data Curation, Formal Analysis, Visualization, Writing - Original Draft; **Junyan Li (Corresponding Author):** Conceptualization, Funding Acquisition, Resources, Supervision, Writing - Review & Editing; **Shuaiyu Liang:** Data Curation, Investigation; **Zhishuncheng Li:** Formal Analysis; **Huimin Tang:** Validation; **Junhong Zhou:** Visualization; **Ping Ning:** Supervision.

Availability of data and materials

All data generated or analyzed during this study are included in this published article.

Ethical Approval: Not applicable

Consent to participate: Not applicable

Consent to publish: Not applicable

References

1. Abdel-Rahman M, Feng X, Muir M, Ghale K, Xu Y, Trenary M (2019): Reaction pathways for HCN on transition metal surfaces. Phys Chem Chem Phys 21, 5274-5284
2. Aliaga MJ, Ramon DJ, Yus M (2010): Impregnated copper on magnetite: an efficient and green catalyst for the multicomponent preparation of propargylamines under solvent free conditions. Org Biomol Chem 8, 43-6
3. Aono H, Hirazawa H, Naohara T, Maehara T, Kikkawa H, Watanabe Y (2005): Synthesis of fine magnetite powder using reverse coprecipitation method and its heating properties by applying AC magnetic field. Materials Research Bulletin 40, 1126-1135
4. Brüger A, Fafilek G, Neumann-Spallart M (2020): Treatment of cyanide: Photoelectrocatalytic degradation using TiO2 thin film electrodes and influence of volatilization. Solar Energy 205, 74-78
5. Cano R, Yus M, Ramón DJ (2012): Impregnated copper or palladium–copper on magnetite as catalysts for the domino and stepwise Sonogashira-cyclization processes: a straightforward synthesis of benzo[b]furans and indoles. Tetrahedron 68, 1393-1400
6. Crundwell FK (2016): The mechanism of dissolution of minerals in acidic and alkaline solutions: Part V surface charge and zeta potential. Hydrometallurgy 161, 174-184

7. Gawande MB, Branco PS, Varma RS (2013): Nano-magnetite (Fe3O4) as a support for recyclable catalysts in the development of sustainable methodologies. Chem Soc Rev 42, 3371-93
8. Hong M, Zhang L, Tan Z, Huang Q (2019): Effect mechanism of biochar's zeta potential on farmland soil's cadmium immobilization. Environ Sci Pollut Res Int 26, 19738-19748
9. Huong DT, Van Tu N, Anh DTT, Tien NA, Ngan TTK, Van Tan L (2021): Removal of Phenol from Aqueous Solution Using Internal Microelectrolysis with Fe-Cu: Optimization and Application on Real Coking Wastewater. Processes 9
10. Li T, Wang Z, Yuan B, Ye C, Lin Y, Wang S, Sha Qe, Yuan Z, Zheng J, Shao M (2021a): Emissions of carboxylic acids, hydrogen cyanide (HCN) and isocyanic acid (HNCO) from vehicle exhaust. Atmospheric Environment 247
11. Li X, Jia Y, Qin Y, Zhou M, Sun J (2021b): Iron-carbon microelectrolysis for wastewater remediation: Preparation, performance and interaction mechanisms. Chemosphere 278, 130483
12. Li Y, Sarathy SM (2020): Probing hydrogen–nitrogen chemistry: A theoretical study of important reactions in NxHy, HCN and HNCO oxidation. International Journal of Hydrogen Energy 45, 23624-23637
13. Liu N, Ning P, Sun X, Wang C, Song X, Wang F, Li K (2021): Simultaneous catalytic hydrolysis of HCN, COS and CS2 over metal-modified microwave coal-based activated carbon. Separation and Purification Technology 259
14. Meng J, Yang G, Yan L, Wang X (2005): Synthesis and characterization of magnetic nanometer pigment Fe3O4. Dyes and Pigments 66, 109-113
15. Nguyen TT, Park HJ, Kim JY, Kim HE, Lee H, Yoon J, Lee C (2013): Microbial inactivation by cupric ion in combination with H2O2: role of reactive oxidants. Environ Sci Technol 47, 13661-7
16. Nikazar M, Alizadeh M, Lalavi R, Rostami MH (2014): The optimum conditions for synthesis of Fe3O4/ZnO core/shell magnetic nanoparticles for photodegradation of phenol. IRANIAN JOURNAL OF ENVIRONMENTAL HEALTH SCIENCE & ENGINEERING 12, 21-27
17. Öğütveren ÜB, Törü E, Koparal S (1999): Removal of cyanide by anodic oxidation for wastewater treament. Water Research 33, 1851-1856
18. Shi LB, Wang YP, Dong HK (2015): First-principle study of structural, electronic, vibrational and magnetic properties of HCN adsorbed graphene doped with Cr, Mn and Fe. Applied Surface Science 329, 330-336
19. Siddiqui H, Qureshi MS, Haque FZ (2016): Surfactant assisted wet chemical synthesis of copper oxide (CuO) nanostructures and their spectroscopic analysis. Optik 127, 2740-2747
20. Tan H, Wang X, Wang C, Xu T (2009): Characteristics of HCN Removal Using CaO at High Temperatures. Energy & Fuels 23, 1545–1550
21. Vijayakumar R, Koltypin Y, Felner I, Gedanken A (2000): Sonochemical synthesis and characterization of purenanometer-sized Fe3O4 particles. Materials Science & Engineering A 286, 101-105

22. Wang B, Sheng H, Shi Y, Song L, Zhang Y, Hu Y, Hu W (2016a): The influence of zinc hydroxystannate on reducing toxic gases (CO, NO(x) and HCN) generation and fire hazards of thermoplastic polyurethane composites. J Hazard Mater 314, 260-269
23. Wang Y, Feng M, Liu Y (2016b): Treatment of Dye Wastewater by Continuous Iron-Carbon Microelectrolysis. Environmental Engineering Science 33, 333-340
24. Xiao Y, Shao Y, Luo M, Ma L-l, Xu D-d, Wu M-h, Xu G (2021): Optimized Study and Column Experiments on Treatment Process of Metronidazole Pharmaceutical Wastewater by Microelectrolysis and Fenton Oxidation. Water, Air, & Soil Pollution 232
25. Xie R, Wu M, Qu G, Ning P, Cai Y, Lv P (2018): Treatment of coking wastewater by a novel electric assisted micro-electrolysis filter. J Environ Sci (China) 66, 165-172
26. Yin L, Song Z, Chang M, Zhang Q, Zhao B, Ning P (2021): Synergetic effect between Fe and Ti species on Fe-Ti-Ox for hydrogen cyanide purification. Environ Technol, 1-7
27. Zhang H, Li L, Hao M, Chen K, Lu Y, Qi J, Chen W, Ren L, Cai X, Chen C, Liu Z, Zhao B, Li Z, Hou P (2021): Yixin-Fumai granules improve sick sinus syndrome in aging mice through Nrf-2/HO-1 pathway: A new target for sick sinus syndrome. J Ethnopharmacol 277, 114254
28. Zhou W, Zhang Y, Li W, Jia H, Huang H, Li B (2019): Adsorption isotherms, degradation kinetics, and leaching behaviors of cyanogen and hydrogen cyanide in eight texturally different agricultural soils from China. Ecotoxicol Environ Saf 185, 109704
29. Zhu X, Mao Y, Liu H, Kang H, Liu B, Song Z, Liu X, Guo Y, Du H, Zhang Q (2019): Cooperative effect of Fe and Ti species over Fe–Ti–Ox catalysts on the catalytic hydrolysis performance of hydrogen cyanide. Applied Organometallic Chemistry 34

Figures

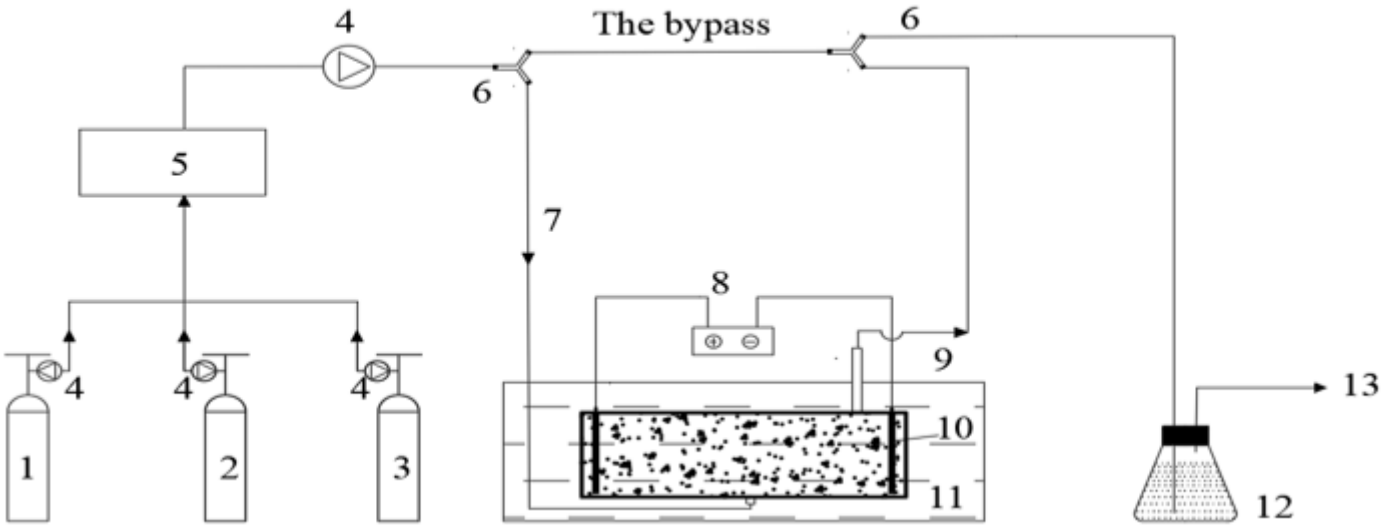

Figure 1

The flowsheet of the experiment

1-Hydrogen cyanide; 2-Nitrogen cyanide; 3-Oxygen cyanide; 4-gas flow meter

5-Gas mixing tank; 6-Glass tee; 7-Air inlet defection; 8-power supply; 9-Gas exhaust;10-electrode

11-Constant temperature water bath; 12-Tail gas absorption device;13-exhaust gas emission

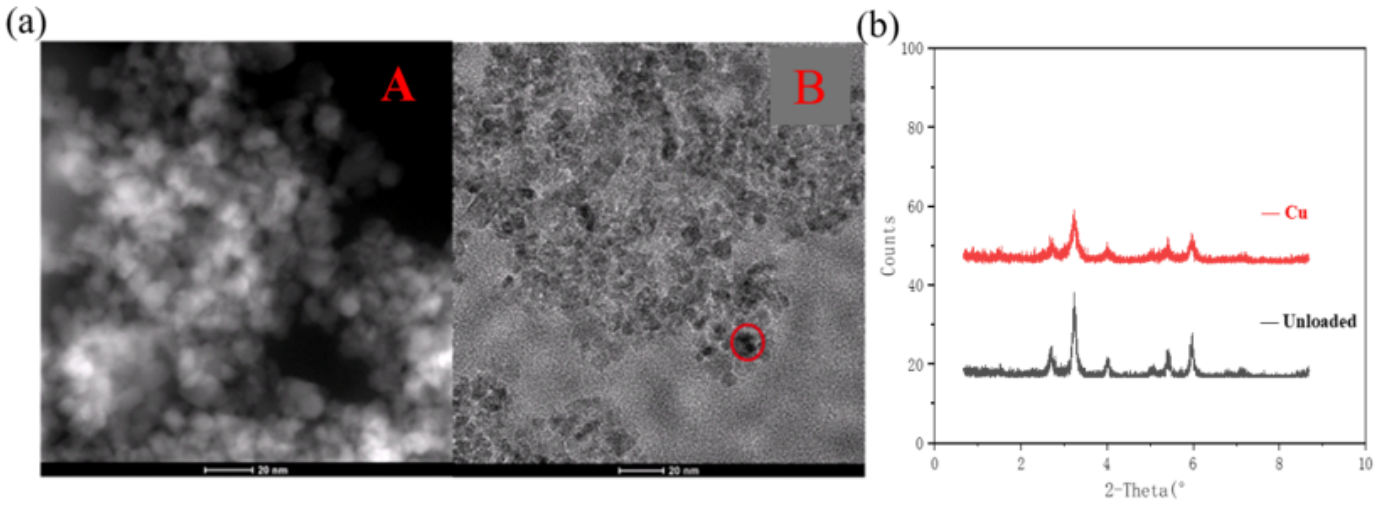

Figure 2

(a) TEM of Fe_3O_4 loaded with Copper (A:Fe_3O_4; B:Cu-Fe_3O_4); (b) XRD of Fe_3O_4 loaded with different components before and after

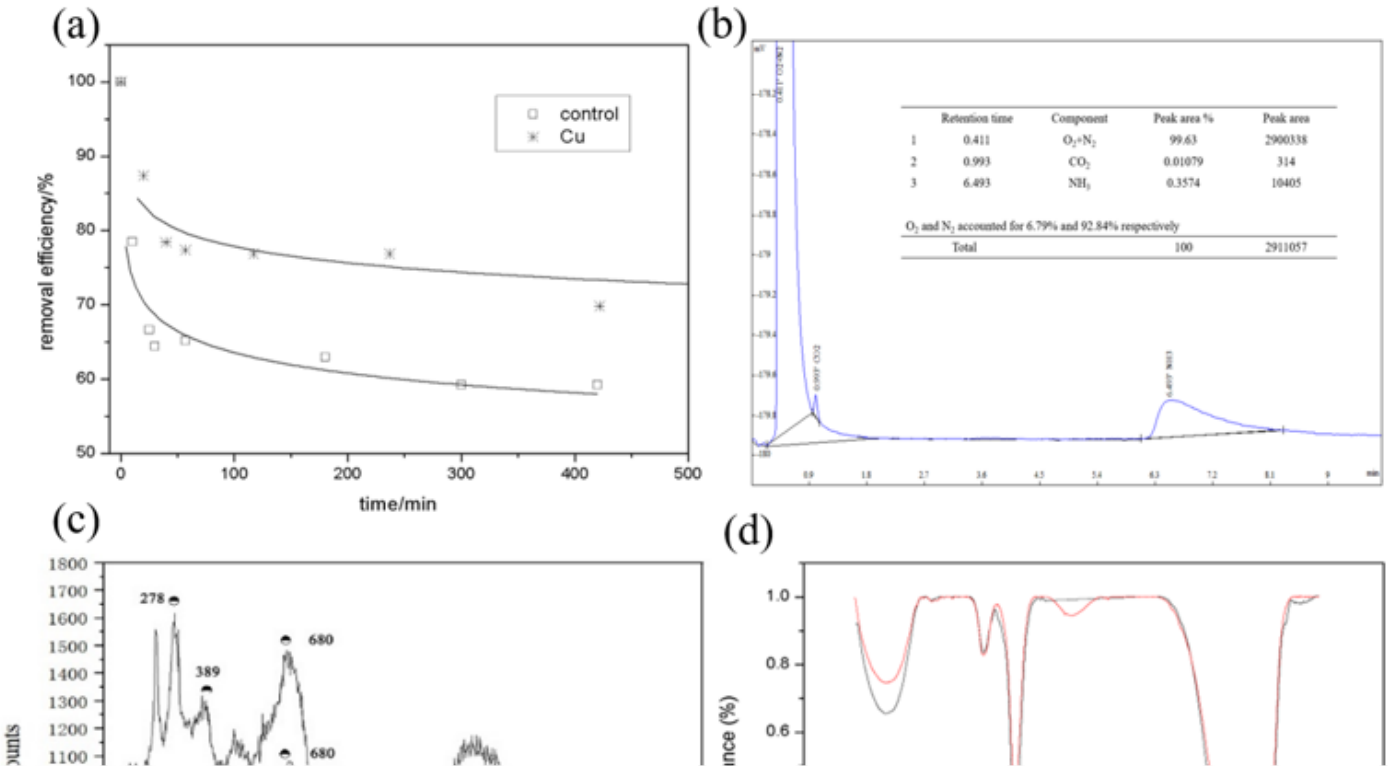

Figure 3

(a)Effect of Cu-Fe_3O_4 on the removal efficiency of HCN Experimental; (b)Gas chromatography of products after purification of HCN with Cu/Fe_3O_4; (c)Comparison of IF spectra of liquid before and after reaction; (d) Raman spectrum of magnetic particles before and after reaction：A: Fe_3O_4 B: Cu-Fe_3O_4 after static removal of HCN

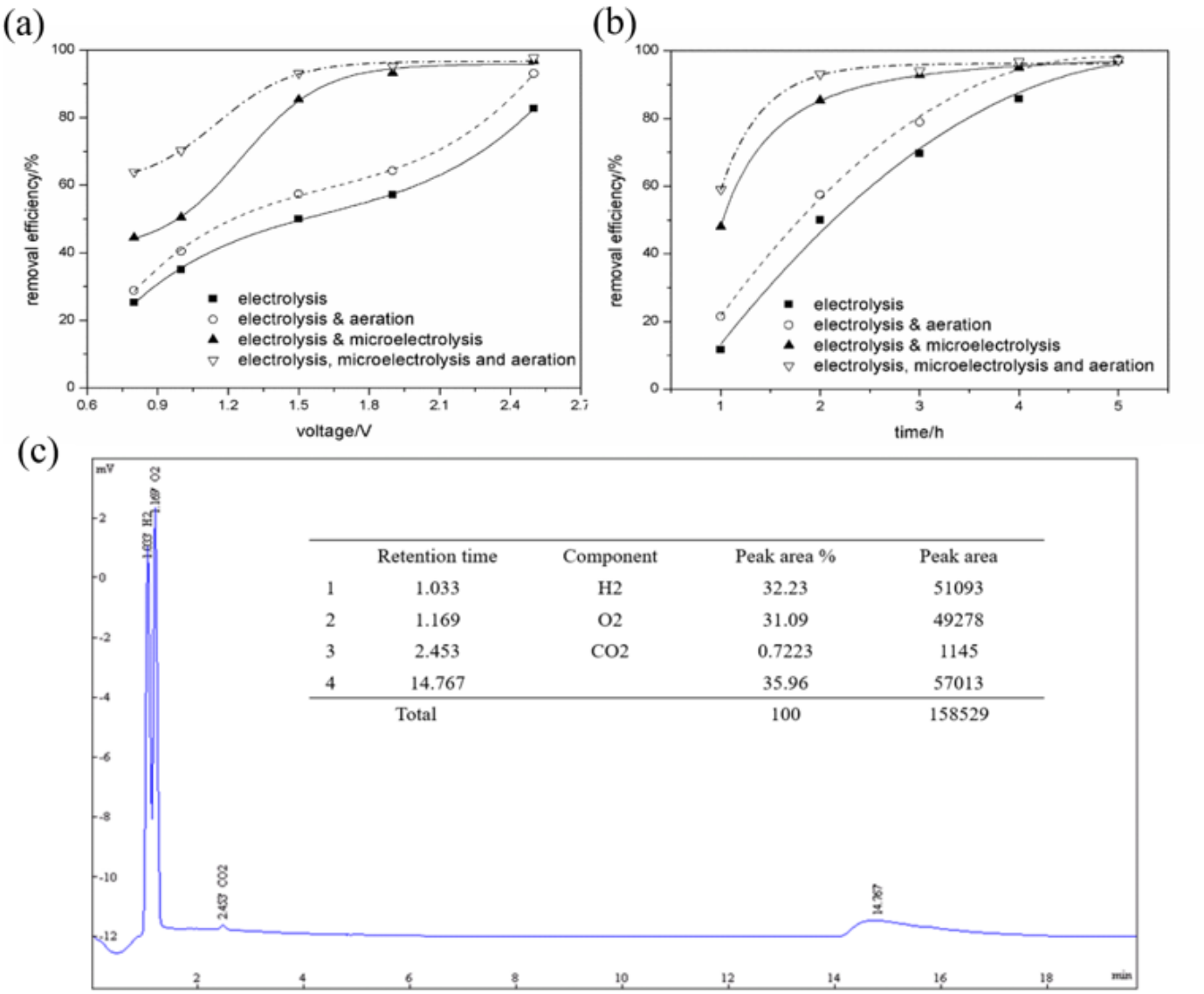

	Retention time	Component	Peak area %	Peak area
1	1.033	H2	32.23	51093
2	1.169	O2	31.09	49278
3	2.453	CO2	0.7223	1145
4	14.767		35.96	57013
	Total		100	158529

Figure 4

(a) Effect of voltage on removal rate under the condition of different combination; (b) Change of removal rate with time under different conditions; (c)The chromatographic results of micro electrolysis gaseous product

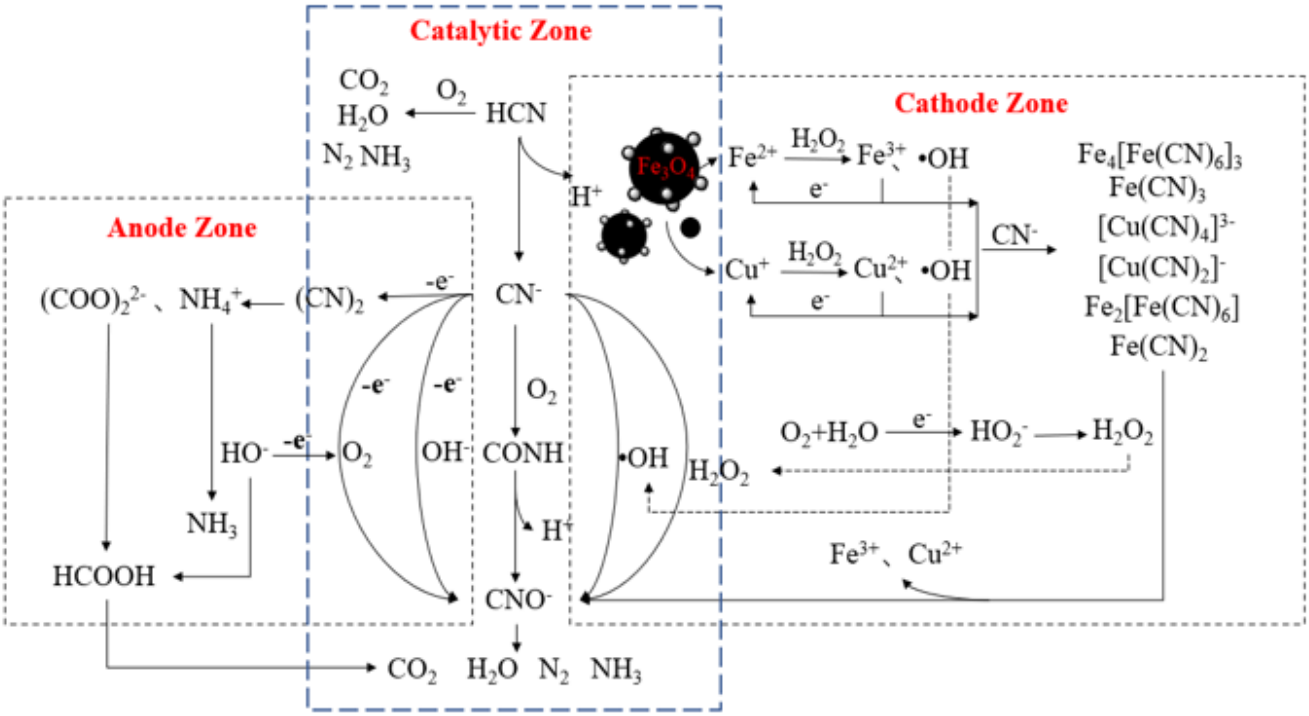

Figure 5

Unit reaction mechanism diagram of electrochemical synergistic Microelectrolysis of Cu-Fe_3O_4 magnetic nanoparticles